Inorganic Chemistry

Article

Solvothermal Metal Azide Decomposition Routes to Nanocrystalline Metastable Nickel, Iron, and Manganese Nitrides

Jonglak Choi and Edward G. Gillan*

Department of Chemistry and the Nanoscience and Nanotechnology Institute, University of Iowa, Iowa City, Iowa 52242

This paper describes the use of solvothermally moderated metal azide decomposition as a route to nanocrystalline mid to late transition metal nitrides. This method utilizes exothermic solid-state metathesis reaction precursor pairs, namely, metal halides ($NiBr_2$, $FeCl_3$, $MnCl_2$) and sodium azide, but conducts the metathesis reaction and azide decomposition in superheated toluene. The reaction temperatures are relatively low (<300 °C) and yield thermally metastable nanocrystalline hexagonal Ni_3N and Fe_2N, and tetragonal MnN. These solvothermally moderated metal nitride metathesis reactions require several days to produce high yields of the intended nitrides. The products are aggregated nanoparticulates with room temperature magnetic properties consistent with their known bulk structures, for example, Fe_2N and Ni_3N are known ferromagnets. The stirred reactions with dispersed fine reagent powders benefit from solvothermal moderation more effectively than submerged pressed reagent pellets. Pellet reactions produced manganese nitrides with lower nitrogen content and higher aggregation than loose powder reactions, consistent with the occurrence of significant local exothermic heating in the pellet metathesis reactions.

Introduction and Background

A wide variety of inorganic materials are derived from reactions between metals and non-oxide light elements, such as B, C, and N. In general, observed metal nitride phases range from nearly stoichiometric MN systems for the main group and early transition series (e.g., GaN and ZrN) to metal-rich structures for the late transition metals (e.g., Cu_3N and Ni_4N). Many early transition-metal nitrides (Groups 3 to 6) are thermally stable, refractory materials, while mid to late transition metals such as manganese, iron, nickel, and copper form somewhat thermally metastable nitrides (dec below ∼500 °C) with a variety of metal-rich phases (e.g., M_2N and M_4N) that can exhibit cooperative magnetic properties. Because of their low thermal stability, the synthesis of bulk powders and nanocrystals of binary mid to late transition-metal nitrides is difficult, and they are most often studied as a component in more thermodynamically stable ternary $M_xM'_yN_z$ systems that are synthesized at relatively high temperatures (e.g., $FeWN_2$, Ni_2Mo_3N, and $Ni_{2−x}Co_xMo_3N$).[1] Transition metals are proposed as magnetic dopants for semiconducting nitrides to enhance their data

storage potential. Several proposed or investigated doped metal nitride systems include Ga−M−N (M = Mn, Fe, Cr) and In−Fe−N.[2]

Metal nitride powders and films are conventionally produced using metals, metal halides, or metal oxides that are thermally converted to nitrides using high-temperature treatment with N_2 or NH_3 usually in excess of 750 °C. Activating nitrogen sources, such as by microwave radiation, enhance binary and ternary nitride reactions using metal oxide precursors.[3] Metal nitrides have also been produced from metal-amine precursors.[4] Successful syntheses of mid

(1) (a) Bem, D. S.; Lampe-Onnerud, C. M.; Olsen, H. P.; zur Loye, H. C. *Inorg. Chem.* **1996**, *35*, 581. (b) Weil, K. S.; Kumta, P. N.; Grins, J. *J. Solid State Chem.* **1999**, *146*, 22. (c) Korlann, S.; Diaz, B.; Bussell, M. E. *Chem. Mater.* **2002**, *14*, 4049. (d) Alconchel, S.; Sapiña, F.; Beltran, D.; Beltran, A. *J. Mater. Chem.* **1999**, *9*, 749. (e) Prior, T. J.; Battle, P. *J. Solid State Chem.* **2003**, *172*, 138. (f) Niewa, R.; DiSalvo, F. J. *Chem. Mater.* **1998**, *10*, 2733. (g) Niewa, R.; Jacobs, H. *Chem. Rev.* **1996**, *96*, 2053.

(2) (a) Decleva, P.; Ohno, M. *Chem. Phys.* **1992**, *160*, 341. (b) Dietl, T.; Ohno, H.; Matsukura, F.; Cibert, J.; Ferrand, D. *Science* **2000**, *287*, 1019. (c) Lukashev, P.; Lambrecht, W. R. L. *J. Appl. Phys.* **2005**, *97*, 10D309/1. (d) Lukashev, P.; Lambrecht, W. R. L. *Phys. Rev. B* **2004**, *70*, 245205. (e) Gosk, J.; Zajac, M.; Byszewski, M.; Kaminska, M.; Szczytko, J.; Twardowski, A.; Strojek, B.; Podsiadlo, S. *J. Supercond.* **2003**, *16*, 79. (f) Park, S. E.; Lee, H.-J.; Cho, Y. C.; Jeong, S.-Y.; Cho, C. R.; Cho, S. *Appl. Phys. Lett.* **2002**, *80*, 4187. (g) Hashimoto, M.; Zhou, Y.-K.; Kanamura, M.; Asahi, H. *Solid State Commun.* **2002**, *122*, 37.

* To whom correspondence should be addressed. E-mail: edward-gillan@uiowa.edu.

to late transition-metal nitrides (M_xN $x > 1$) are generally accomplished using metal-ammonia complexes or metal amine precursors that are converted to crystalline metal nitrides via elevated temperature reactions with gaseous or supercritical ammonia, including Co_3N,[5] Ni_3N,[5,6] and Cu_3N.[5,7] Thin films of several metal-rich nitrides, most commonly Cu_3N, have also been produced by metal or metal precursor reactions with nitrogen plasmas or ammonia.[8] Iron nitrides have also been synthesized from reactive iron nanoparticles and ammonia below 400 °C.[9]

Thermally stable nanocrystalline metal nitrides have been synthesized from solid-state metathesis (SSM) reactions using reactive solid nitrogen sources such as Li_3N, Mg_3N_2, and NaN_3.[10] The SSM approach has wide applicability and flexibility, but the highly exothermic nature of such rapidly propagating systems makes it difficult to isolate thermally sensitive (metastable) nitrides. Since SSM reactions often reach very high transient temperatures ($\sim$1300 °C), they usually produce thermodynamically stable metal nitrides. We recently demonstrated that non-aqueous superheated toluene is a viable reaction medium for the synthesis of GaN at 260 °C via decomposition of energetic metal azide precursors derived from SSM-style reactions.[11] The solvent moderates energetic decomposition processes, and the azide precursor intermediates convert at temperatures below 300 °C to nitride structures, including thermally metastable nanocrystalline InN[12] and Cu_3N[13] powders, which decompose below 500 °C. Selected other precedents for the solvothermal synthesis of thermally stable metal nitrides using reactive Li_3N or NaN_3 precursors are nanocrystalline TiN powders from superheated benzene at 380 °C[14] and nanocrystalline GaN in benzene at 280 °C.[15] Recent studies using solvothermal formation and decomposition of $M-NH_2$ intermediates formed from SSM precursor reactions demonstrated the direct synthesis of crystalline TaN nanoparticulate materials.[16]

Increasing the materials chemist's synthetic toolkit with new and flexible solvothermal approaches to crystalline transition metal nitrides will facilitate further studies on synthesis of new metastable nanoparticulate metal nitride stoichiometries, including metal-doped semiconducting nitrides. This current study demonstrates that several thermally metastable nanocrystalline mid to late transition metal nitrides are accessible in superheated toluene solvents from in situ produced energetic metal azide intermediates. The synthesis and characterization of Ni_3N, Fe_2N, and $Mn-N$ materials are described below.

Experimental Section

Solvothermal Reaction Considerations. The synthetic approach and precautions used in the present studies are similar to those of our previously published metal azide to metal nitride solvothermal chemistry.[12,13] Toluene ($C_6H_5CH_3$, Fisher Scientific, certified) used for the solvothermal reactions was dried over sodium and distilled under N_2. Methanol (Fisher, 99.9%, anhydrous H_2O <0.01%) was used as received and degassed with N_2 gas prior to use. The general synthetic method involves reactions of a metal halide (MX_n, M = Ni, Fe, Mn; X = Br, Cl) with NaN_3 that were balanced so the molar ratio of metal halide to NaN_3 used is 1 to 2 for dihalide (1 to 3 for trihalide) reactions to ensure that all halide is ideally sequestered as NaX. The anhydrous metal halide and NaN_3 solids were separately ground to fine powders with a mortar and pestle in an argon-filled glovebox (Vacuum Atmospheres MO-40M) and loaded into a high-temperature, high-pressure stainless steel reactor (125 mL, Parr Instruments Model 4752, 3000 psi limit). The reactor with the powdered reagent mixture and a Teflon-coated stirbar was capped with a septum, removed from the glovebox, and partially filled with N_2 degassed toluene ($\sim$85 mL or 77% of the reactor volume) using inert atmosphere Schlenk techniques. The reactor was then mated with its high-pressure head, sealed under a flow of nitrogen gas, and placed in a beaker-shaped Glas-Col heating mantle where it was slowly heated with constant stirring using an external magnetic stirrer. The reported reaction temperatures were measured by an internal reactor thermocouple that was submerged in the solvent and about one inch from the bottom of the reactor. Slow heating ramps were chosen to avoid rapid exothermic degradation of metal azide intermediates, which could lead to product decomposition. Onset and degree of azide decomposition was monitored by gas evolution rates using the reactor's analog pressure gauge. Increases in reaction temperature were made after the vessel reached a pressure plateau, which usually occurred within a few hours of raising the temperature. Temperature ramp rates were adjusted based on pressure changes due to nitrogen gas evolution. The maximum reaction temperature was determined as the point where gas evolution ceased, which indicated that the azide precursor had completely decomposed.

Safety Note. Caution! *Metal azides are often thermally unstable and shock sensitive. Care should be taken whenever working with reactions that produce azides as products or intermediates. Reactions should be performed on small scales in high-pressure*

(3) (a) Houmes, J. D.; zur Loye, H.-C. *J. Solid State Chem.* **1997**, *130*, 266. (b) Vaidhyanathan, B.; Rao, K. J. *Chem. Mater.* **1997**, *9*, 1196. (c) Gerardin, D.; Morniroli, J. P.; Michel, H.; Gantois, M. *J. Mater. Sci.* **1981**, *16*, 159.

(4) (a) Wu, C.; Li, T.; Hu, S.; Xie, Y. *New J. Chem.* **2005**, *29*, 1610. (b) Xiao, J.; Xie, Y.; Tang, R.; Luo, W. *Inorg. Chem.* **2003**, *42*, 107. (c) Mazumder, B.; Hector, A. L. *J. Mater. Chem.* **2008**, *18*, 1392. (d) Hwang, J.-W.; Campbell, J. P.; Kozubowski, J.; Hanson, S. A.; Evans, J. F.; Gladfelter, W. L. *Chem. Mater.* **1995**, *7*, 517.

(5) Desmoulins-Krawiec, S.; Aymonier, C.; Loppinet-Serani, A.; Weill, F.; Gorsse, S.; Etourneau, J.; Cansell, F. *J. Mater. Chem.* **2004**, *14*, 228.

(6) (a) Leineweber, A.; Jacobs, H.; Hull, S. *Inorg. Chem.* **2001**, *40*, 5818. (b) Gajbhiye, N. S.; Ningthoujam, R. S. *J. Phys. Stat. Sol. A* **2002**, *189*, 691. (c) Juza, R.; Sachsze, W. *Z. Anorg. Allg. Chem.* **1943**, *251*, 201.

(7) Zachwieja, U.; Jacobs, H. *J. Less Common Met.* **1990**, *161*, 175.

(8) (a) Maya, L. *J. Vac. Sci. Technol. A* **1993**, *11*, 604. (b) Borsa, D. M.; Boerma, D. O. *Surf. Sci.* **2004**, *548*, 95. (c) Pierson, J. F. *Vacuum* **2002**, *66*, 59. (d) Nosaka, T.; Yoshitake, M.; Okamoto, A.; Ogawa, S.; Nakayama, Y. *Thin Solid Films* **1999**, *348*, 8. (e) Soto, G.; Diaz, J. A.; de la Cruz, W. *Mater. Lett.* **2003**, *57*, 4130. (f) Pinkas, J.; Huffman, J. C.; Baxter, D. V.; Chisholm, M. H.; Caulton, K. G. *Chem. Mater.* **1995**, *7*, 1589.

(9) (a) Koltypin, Y.; Cao, X.; Prozorov, R.; Balogh, J.; Kaptas, D.; Gedanken, A. *J. Mater. Chem.* **1997**, *7*, 2453. (b) Han, Y.; Wang, H.; Zhang, M.; Su, M.; Li, W.; Tao, K. *Inorg. Chem.* **2008**, *47*, 1261.

(10) (a) Gillan, E. G.; Kaner, R. B. *Inorg. Chem.* **1994**, *33*, 5693. (b) Hector, A. L.; Parkin, I. P. *Polyhedron* **1995**, *14*, 913. (c) Parkin, I. P. *Chem. Soc. Rev.* **1996**, 199. (d) Gillan, E. G.; Kaner, R. B. *Chem. Mater.* **1996**, *8*, 333.

(11) Grocholl, L.; Wang, J.; Gillan, E. G. *Chem. Mater.* **2001**, *13*, 4290.

(12) Choi, J.; Gillan, E. G. *J. Mater. Chem.* **2006**, *16*, 3774.

(13) Choi, J.; Gillan, E. G. *Inorg. Chem.* **2005**, *44*, 7385.

(14) Hu, J.; Lu, Q.; Tang, K.; Yu, S.; Qian, Y.; Zhou, G.; Liu, X. *J. Am. Ceram. Soc.* **2000**, *83*, 430.

(15) Xie, Y.; Qian, Y.; Wang, W.-Z.; Zhang, S.; Zhang, Y. *Science* **1996**, *272*, 1926.

(16) Mazumder, B.; Chirico, P.; Hector, A. L. *Inorg. Chem.* **2008**, *47*, 9684.

vessels with safety release valves. Use proper protection and extreme caution when working with undecomposed metal azide intermediates. Solid metal azides may detonate upon rapid heating, vigorous grinding or stirring, and by friction from spatula scraping.

Nickel Nitride Synthesis. A typical nickel nitride synthesis utilized $NiBr_2$ (3.02 g, 13.8 mmol, Alfa Aesar, 99%) and NaN_3 (1.80 g, 27.6 mmol, Aldrich, 98%). NaN_3 was used as received, but it was necessary to dry $NiBr_2$ by heating at 200 °C under dynamic vacuum prior to use, since small amounts of adventitious surface hydration present on commercial "anhydrous" metal halides lead to measurable crystalline NiO in the final product. The nickel nitride precursors were heated to ~100 °C (11 °C/hr, 3 h hold), then ramped to ~120 °C (5 °C/hr, ~17 h hold), and then ramped to ~170 °C (4 h hold) to facilitate the synthesis of metal azide intermediates. No significant pressure increases above the solvent background were observed at this point. Subsequent temperature increases were made over 4 days (~20 °C/day) to facilitate the moderate (non-explosive) nickel azide decomposition. The maximum nickel nitride reaction temperature of 260 °C was typically maintained for a day, leading to a total solvothermal reaction time of approximately 6 days.

Iron Nitride Synthesis. A typical iron nitride synthesis utilized $FeCl_3$ (2.02 g, 12.5 mmol, Alfa Aesar, 98%) and NaN_3 (2.43 g, 37.4 mmol), which were heated from room temperature to ~90 °C (60 °C/hr, 3 h hold) to facilitate the synthesis of metal azide intermediates. No significant pressure increases above the solvent background were observed at this point. Subsequent temperature increases were made over 3 days (~50 °C/day) up to 240 °C to facilitate non-explosive azide decomposition. The reaction mixture was then heated at up to ~270 °C over 3 days (10 °C/day, 20 h hold). During this final heating stage, the pressure more significantly changed with small increments of temperature. The total solvothermal reaction time was about 7 days. For the comparison purposes, an iron nitride reaction was performed using a faster reaction heating ramp to 240 °C (~15 °C/hr, 3 h hold), before ramping to 270 °C in ~ 1 h (29 h hold). The total reaction time for this fast ramp reaction was 2 days.

Manganese Nitride Synthesis. A typical manganese nitride precursor reaction using $MnCl_2$ (3.00 g, 23.8 mmol, Cerac, 99.5%) and NaN_3 (3.10 g, 47.6 mmol) was heated to ~70 °C (4 h hold) and then raised to ~220 °C (20 °C/hr, 1 day hold) to facilitate the synthesis of metal azide intermediates. No significant pressure increases above the solvent background were observed at this point. Subsequent temperature increases in ~5 to 10 °C increments were made over 3 days from 224 °C, where a significant pressure increase was first detected, up to 280 °C (~20 °C/day). The temperature was then raised to 290 °C (5 °C/day, 3 d hold). The total reaction time was approximately 6 days.

In an exploratory static solvothermal experiment, $MnCl_2$ and NaN_3 were separately ground with a mortar and pestle, intimately mixed together, and then pressed into 15 pellets (total reagent mass was ~33% of that used in the stirred reaction described above) using an IR pellet press in the glovebox. Each pellet had a disk shape (~7.5 mm diameter, 2 mm thickness). The pellets were stacked inside the reactor and submerged in the toluene solvent. The pressed pellets were slowly heated to 220 °C (~ 10 °C/hr, 6 h hold), followed by ~10 °C increments up to 240 °C (15 h hold). Some rapid pressure increases were recorded around 230 °C and later near 255 °C for these pellets. The temperature was then raised to 290 °C (~50 °C/day, 3 day hold), resulting in a nearly 6 day total reaction time.

Metal Nitride Product Isolation and Annealing Studies. After the reactors were cooled to room temperature, the headspace gases were sampled by gas phase IR, and the reaction solution was removed under inert conditions using Schlenk transfer techniques. The as-synthesized solid was dried under vacuum and transferred to an argon-filled glovebox. The byproduct NaCl or NaBr and unreacted precursors were removed from finely ground samples by dissolution in degassed methanol under inert N_2 conditions. The washed solid was filtered using air-free Schlenk techniques, dried under vacuum, and stored in a glovebox. If residual sodium halide was detected by X-ray diffraction, the samples were rewashed with methanol.

Selected as-synthesized and washed products were annealed at elevated temperatures (300−500 °C) in sealed, evacuated glass ampules for various lengths of time, typically 1−2 days. These annealing studies were performed to investigate the phase and structural thermal stability of as-synthesized metal nitrides and to determine whether their crystallinity could be improved by annealing.

Characterization of Nitride Products. The phase and crystallinity of the products were analyzed by powder X-ray diffraction (XRD) using a Siemens D5000 diffractometer (50 kW, 30 mA, 0.03°/step, and 3−5 s/step count times, silicon or NaCl internal standards). Nitride lattice parameters were determined by least-squares refinement, and average crystallite sizes were calculated from several nitride peaks in the 20−50° two-theta region using the Scherrer and Warren equations.[17] Unit cell structures, simulated powder XRD patterns, and lattice parameter refinements were generated using Powder Cell 2.3 (http://www.ccp14.ac.uk/) computer program. FT-IR spectra were taken on a Nicolet Nexus 670 spectrometer in transmission mode using KBr pellets for solids or a 10 cm path length cell with NaCl windows for gases. Thermogravimetric-differential thermal analysis (TG-DTA) experiments were performed on a Seiko Exstar TG-DTA 6300 system under flowing argon or air with a 5−10 °C/min heating ramp. Metal contents in the products were determined thermogravimetrically by converting the metal nitrides to metal oxides. Bulk elemental CHN combustion analysis was obtained from Desert Analytics (www.desertanalytics.com) or a Perkin-Elmer CHN Analysis instrument (PE 2400 Series II CHNS/O analyzer). Scanning electron microscopy (SEM) information was obtained with a Hitachi S-4000 field emission system (5 kV) on powders affixed to aluminum or carbon holders. This system includes an IXRF X-ray microanalysis system for energy dispersive spectroscopy that provided semiquantitative information on the metal, sodium, bromine/chlorine ratios in the washed or annealed samples. Transmission electron microscopy (TEM) information was obtained with a JEOL JEM-1230 TEM at 100 kV. Samples were sonicated in a MeOH solution for approximately 2 h and deposited onto Formvar coated copper TEM grids. Surface X-ray photoelectron spectroscopy (XPS) was performed on powders embedded in indium foil using a Kratos Axis Ultra instrument (Al Kα radiation). Semiquantitative analysis was obtained using the CasaXPS software package (www.casaxps.com). Room-temperature magnetic susceptibility measurements were obtained on a Johnson-Matthey MKS-Auto (Mark II) benchtop magnetic susceptibility balance. Highly magnetic samples were diluted with a known amount of NaCl powder prior to analysis so measurements were within the instrument's range. Sample gram susceptibility was converted to molar values (cm^3/mol) and corrected for diamagnetic contributions, assuming that the product mass consisted entirely of the identified crystalline nitride phase.

(17) Warren, B. E. *X-Ray Diffraction*; Dover Publications, Inc.: New York, 1990.

Results and Discussion

Metal Azide to Metal Nitride Solvothermal Reactions.
As noted in the introduction, stable gaseous nitrogen precursors such as N_2 and NH_3 usually require high reaction temperatures to convert metal precursors into metal nitrides. Reactive metal azide precursor decomposition in pressurized superheated organic solvent reactions can lead to reduced metal nitride synthesis temperatures and permits access to nanocrystalline metal nitrides that are thermally metastable and difficult to synthesize using conventional solid-state methods. The current study demonstrates the synthesis of metal nitrides from reactions of sodium azide [NaN_3 ΔH_f = +21.3 kJ/mol] and anhydrous metal halides in superheated toluene. A general balanced reaction for successful solvothermal syntheses is shown in eq 1 (MX_n = $NiBr_2$, $FeCl_3$, or $MnCl_2$).

$$MX_n + nNaN_3 \rightarrow [M(N_3)_n + nNaX] \rightarrow MN_y +$$
$$nNaX + \tfrac{1}{2}(3n-y)N_2 \ (1)$$
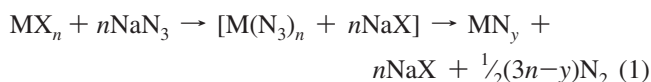
In the superheated toluene, sodium azide transforms metal halides into metal azide intermediates, which are energetic precursors with generally large positive heats of formation (e.g., $Mn(N_3)_2$ ΔH_f = +393 kJ/mol).[18] Metal halogen to azide bond exchange using NaN_3 is common in metal azide formation reactions, and several molecular structures contain sufficiently stable M−N_3 bonds to permit extensive physical characterization.[19] The coformation of an alkali halide byproduct in eq 1 provides a major thermodynamic driving force for metal azide formation (e.g., NaCl ΔH_f = −386 kJ/mol). The intermediate metal azide is likely poorly soluble in toluene and may be embedded in an NaX byproduct matrix where it decomposes with nitrogen gas evolution at higher solvothermal temperatures. Pressure evolution during azide decomposition is a key diagnostic tool that allows us to determine how quickly and how long to heat the metal nitride precursor solutions.

The three metal halide/NaN_3 precursor mixtures react and decompose with gas evolution at similar superheated solvothermal temperatures ($\sim$260−290 °C). While the azide intermediates were not isolated and identified in the current work, our prior studies showed that isolable metal azide intermediates [e.g., $Cu(N_3)_2$ and $Ga(N_3)_n$] form in these solvothermal metathesis reactions.[11,12] Figure 1 shows reactor pressure versus temperature curves for these three metal azide solvothermal reactions. In each case, there is little gas evolution above the toluene background until temperatures reach near 200 °C. The metal azide intermediate's stability, based on the onset of significant gas evolution/azide decomposition, appears to increase from Ni ($\sim$200 °C) to Fe ($\sim$225 °C) to Mn ($\sim$240 °C). These values are in rough agreement
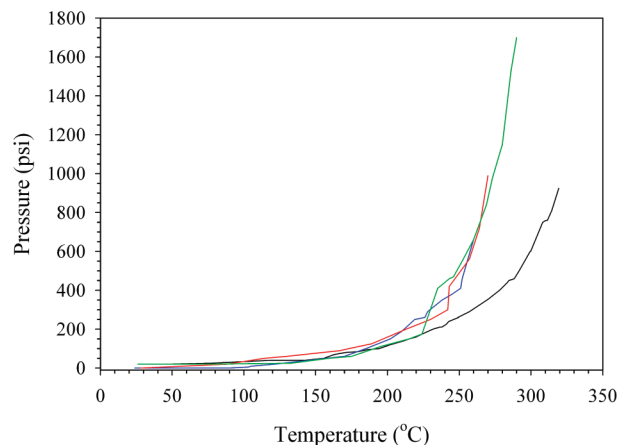

Figure 1. Comparison of pressure evolution observed at different temperatures for the solvothermal reactions between NaN_3 and $NiBr_2$ (blue), $FeCl_2$ (red), or $MnCl_2$ (green) in superheated toluene. The toluene background pressure (black) is plotted for comparison.
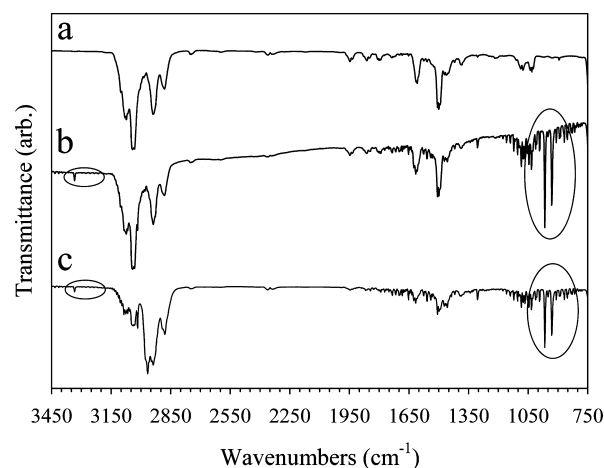

Figure 2. IR comparison of evolved gases from solvothermal superheated toluene reactions between NaN_3 and (a) $NiBr_2$, (b) $FeCl_2$ (red), or (c) $MnCl_2$. Circled regions of (b) and (c) indicate NH_3 vibrations. All peaks in (a) are consistent with toluene IR spectra.

with reported stabilities of $Ni(N_3)_2$ (steady dec at 230 °C),[20] phosphine-coordinated $Fe(N_3)_2$ (dec $\sim$160−170 °C),[21] and $Mn(N_3)_2$ (dec 218 °C).[18]

Upon cooling to the pressurized reactors to room temperature, residual gas pressures generally agreed with predicted N_2 evolution based on a combination of headspace gas and additional dissolved gases in the toluene. The theoretical magnitude of dissolved gas was estimated using Henry's Law calculations for N_2 in an arene solvent. After depressurizing the reactor, effervescent bubbles were frequently observed to evolve from the toluene solution. IR analysis of the pressurized gas in the reactor was consistent with primarily toluene, particularly for Ni_3N (Figure 2). For the Fe and Mn reactions, NH_3 was also observed and its formation indicates that some azide-solvent side reaction occurs during azide decomposition (M−N_3 → M−N + N_2), possibly via hydrogen abstraction from toluene by metal nitrene intermediates. Ammonia is clearly evident in nitride reactions conducted

(18) *Energetic Materials I: Physics and Chemistry of the Inorganic Azides*; Fair, H. D., Walker, R. F., Eds.; Plenum Press: New York, 1977.
(19) (a) Escuer, A.; Aromi, G. *Eur. J. Inorg. Chem.* **2006**, 4721, and references therein. (b) Meyer, F.; Demeshko, S.; Leibeling, G.; Kersting, B.; Kaifer, E.; Pritzkow, H. *Chem.—Eur. J.* **2005**, *11*, 1518. (c) Li, R.-Y.; Wang, X.-Y.; Liu, T.; Xu, H.-B.; Zhao, F.; Wang, Z.-M.; Gao, S. *Inorg. Chem.* **2008**, *47*, 8134. (d) Bonnet, M.-L.; Aronica, C.; Chastanet, G.; Pilet, G.; Luneau, D.; Mathonire, C.; Clrac, R.; Robert, V. *Inorg. Chem.* **2008**, *47*, 1127.

(20) Sood, R. K.; Nya, A. E.; Etim, E. S. *J. Therm. Anal.* **1981**, *22*, 231.
(21) Field, L. D.; George, A. V.; Pike, S. R.; Buys, I. E.; Hambley, T. W. *Polyhedron* **1995**, *14*, 3133.

Table 1. Solvothermal Metal Azide Decomposition Products

reagents[a]	T_{rxn} (°C)	XRD phase (crystallite size) and lattice parameters (Å)	MN_x analysis wt % (M:N:C:H)	M:N molar ratio
$NiBr_2 + 2NaN_3$	260	hexagonal Ni_3N (31 nm) $a = 4.627$; $c = 4.310$	73.6:10.33:3.10:1.15	1:0.59
$FeCl_3 + 3NaN_3$	270	hexagonal Fe_2N (26 nm) $a = 4.809$; $c = 4.428$	48.2:7.84:26.7:5.30	1:0.65
$MnCl_2 + 2NaN_3$	290	tetragonal MnN (20 nm) $a = 4.201$; $c = 4.150$	64.0:12.0:4.5:0.08	1:0.86
$MnCl_2 + 2NaN_3$ pellets	290	tetragonal Mn_3N_2 (18 nm) $a = 2.974$; $c = 12.10$ cubic Mn_4N (29 nm): $a = 3.864$	69.0:9.45:4.93:0.39	1:0.54

[a] Stirred powders unless noted.

at 270 °C or higher, thus undesirable solvent/nitride surface reactions may also occur at elevated temperatures.

The isolated solids from the three metal azide decomposition reactions were washed with anhydrous methanol under inert conditions to remove NaX byproducts. All three nitride products were isolated in mass yields of ~100% or slightly greater, assuming that the amount of metal halide used was converted to the detected crystalline nitride phase (details below). These high values are not surprising since bound surface organics (tolyl and methanol) and azide residues are detected by IR (Supporting Information, Figure S1), consistent with elemental analysis results (Table 1).

Nickel Nitride Products. Previous synthetic approaches to hexagonal Ni_3N films or particles have involved nitridation of nickel powder or molecular precursors with NH_3[6] or NaN_3 under high pressure.[22] Gas−solid reactions often have elemental nickel contamination because of the low thermal stability of the Ni_3N product (dec < 450 °C) relative to required reaction temperatures. Other Ni_2N and Ni_3N_2 phases have only been observed in thin films by DC sputtering in Ar/N_2.[23]

Initial synthetic attempts using anhydrous $NiCl_2$ were unsuccessful, leading to incomplete reactions even at elevated temperatures and yielding reaction products containing significant crystalline NiO contamination. In contrast, vacuum-dried $NiBr_2$ led to more efficient nitride formation reactions. This may be due its higher purity or better solubility in heated toluene than $NiCl_2$. The solvothermal $NiBr_2/NaN_3$ decomposition reaction at 260 °C produced nanocrystalline hexagonal Ni_3N (JCPDS No. 10-280, Figure 3 a, b)[24] with a 31 nm average crystallite size and no detectable crystalline impurities by XRD analysis. Table 1 contains selected synthetic, structural, and compositional information.

As is true of most nanocrystalline materials synthesized from organic solvents, they have hydrocarbon surface coatings. EDS analysis of washed Ni_3N powders shows that bromine and sodium are generally not detectable above baseline noise (<1 wt %). The weight percentages listed in Table 1 are consistent with a slight excess of nitrogen (Ni_3N is 92.6 wt % Ni and 7.4 wt % N with a M:N molar ratio of 1:0.33). The Ni_3N product is black with a greenish surface color, which may correspond to a surface coating of nickel azide, which is a green solid.[18,20] The presence of azide
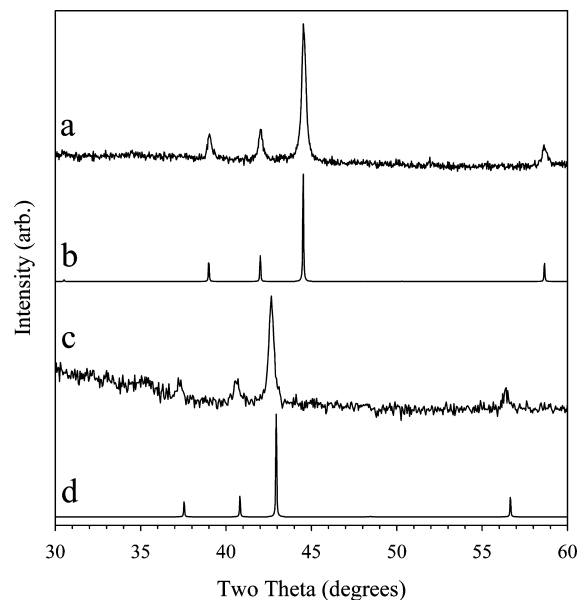

Figure 3. Powder XRD results for (a) Ni_3N from $NiBr_2$ and NaN_3, (b) calculated pattern for hexagonal Ni_3N ($a = 4.616$ Å, $c = 4.298$ Å), (c) Fe_2N from $FeCl_3$ and NaN_3, and (d) calculated pattern for hexagonal Fe_2N ($a = 4.787$ Å, $c = 4.418$ Å).

residues is supported by solid-state IR spectra showing an azide vibration near 2070 cm^{-1}, in addition to an expected Ni−N stretch at 650 cm^{-1} (Supporting Information, Figure S1a).[25] After several months in air, the green surface color fades, and XPS analysis shows that the M:N surface atomic ratios decrease from ~1:0.6 to 1:0.2; however, there are no detectable changes in Ni_3N powder's XRD bulk crystallinity. The TG-DTA of methanol-washed Ni_3N in flowing argon showed ~15% weight loss by 300 °C (organic/azide surface residues) and significant decomposition near 410 °C, producing nickel metal (Supporting Information, Figure S2). A solvothermal $NiBr_2/NaN_3$ reaction that was heated up to 270 °C also showed evidence of crystalline nickel metal formation; thus, the Ni_3N synthesis must be performed significantly below its bulk nitride decomposition temperature.

Iron Nitride Products. Similar to the nickel nitride system, iron nitrides are conventionally synthesized by routes such as iron powder or film reactions with NH_3 or H_2/N_2 gases, often followed by annealing.[26] Iron nitride synthesis is synthetically challenging since the nitride phases (e.g., $Fe_8N \rightarrow FeN$) are thermally metastable with respect to decomposition to iron metal.[27] For example, FeN loses N_2 to form Fe_2N by 320 °C[28] and most metal-rich nitride phases decompose to elemental iron by ~700 °C.[29] Our solvothermal iron azide decomposition reaction produces nanocrys-

(22) Guillaume, C.; Morniroli, J. P.; Frost, D. J.; Serghiou, G. *J. Phys.: Condens. Matter.* **2006**, *18*, 8651.

(23) (a) Dorman, G. J. W. R.; Sikkens, M. *Thin Solid Films* **1983**, *105*, 251. (b) Kawamura, M.; Abe, Y.; Sasaki, K. *Vacuum* **2000**, *59*, 721. (c) Maya, L. *J. Vac. Sci. Technol. A* **1993**, *11*, 604. (d) Juza, R.; Hahn, H. *Z. Anorg. Allg. Chem.* **1938**, *239*, 282.

(24) Villars, P.; Calvert, L. D. *Pearson's handbook of crystallographic data for intermetallic phases*; ASM International: Materials Park, OH, 1991.

(25) Adams, D. M. *Metal-Ligand and Related Vibrations*; St. Martin's Press: New York, 1968.

talline hexagonal Fe_2N (ε-phase, Figure 3c, d)[24] with a ~26 nm average crystallite size. The iron-rich nature of this product made obtaining high quality diffraction difficult since iron absorbs significant incoming copper X-ray radiation.[17]

After the methanol wash, the Fe_2N powder was stable in air at room temperature for over 1 year, as confirmed by XRD where the crystallinity did not degrade and no crystalline impurity phases were observed. The IR spectrum of this washed product indicates that some azide residues remain (2060 cm^{-1}, Supporting Information, Figure S1b), consistent with the slightly higher nitrogen content than the ideal Fe:N molar ratio of 1:0.5. EDS analysis did not detect sodium or chlorine in the washed product, but it contains significant hydrocarbon content (Table 1). TG-DTA analysis (argon flow to 1000 °C, Supporting Information, Figure S2) on the methanol washed Fe_2N yielded a mixture of Fe and Fe_3O_4 (minor). An unwashed Fe_2N product heated under the same conditions yields crystalline iron metal, indicating little or no oxygen contamination is present in the as-synthesized product. TG-DTA analysis showed significant Fe_2N decomposition occurs by 540 °C.

XRD analysis of an unwashed Fe_2N sample subjected to stepwise sealed ampule thermal annealing up to 400 °C indicates that there is nitrogen loss from Fe_2N to $Fe_{2+x}N$ by 300 °C (peaks shift toward higher 2θ angle hexagonal Fe_3N positions, $a = 4.70$ Å, $c = 4.38$ Å),[30] then to Fe_3N by ~350 °C, and finally to Fe_4N along with Fe metal formation after prolonged heating at 350 °C.[31] The Fe_4N phase persists until 400 °C, finally decomposing to iron metal (Supporting Information, Figure S3). These XRD results indicate that the iron nitride is somewhat less thermally stable than phase diagram predictions, which may be due to the nanocrystalline nature of this product and reactions with hydrocarbon impurities.[27b,29]

The effect of heating rate and reaction time on iron nitride formation from $FeCl_3/3NaN_3$ was investigated using a rapid heating profile and short reaction time (~2 days vs 6 days, see Experimental Section). This faster 2 day reaction was heated to the same maximum temperature as the slower 6 day reaction described earlier. The isolated products from this rapid reaction showed evidence of Fe_2N but also crystalline unreacted NaN_3 and reduced $FeCl_2$. The reduced
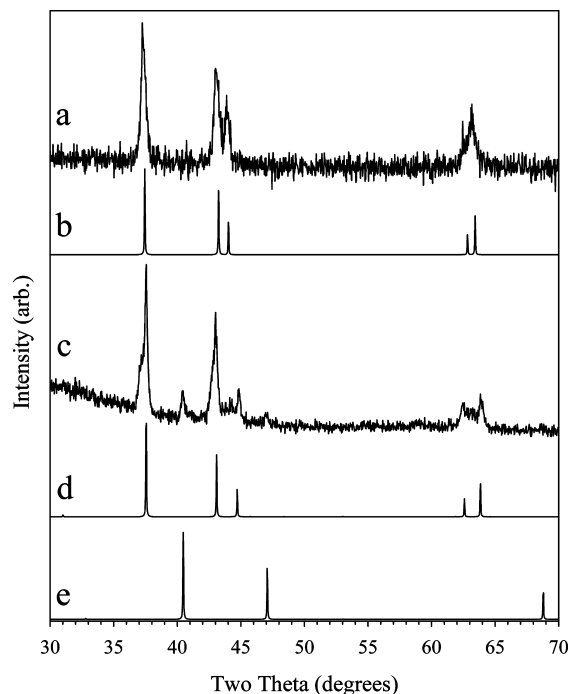

Figure 4. Powder XRD results for (a) MnN from powdered $MnCl_2$ and NaN_3, (b) calculated pattern for tetragonal MnN ($a = 4.18$ Å, $c = 4.11$ Å), (c) Mn_3N_2/Mn_4N mixture from pellet containing $MnCl_2$ and NaN_3, (d) calculated pattern for tetragonal Mn_3N_2 ($a = 2.966$ Å, $c = 12.15$ Å), and (e) calculated pattern for cubic Mn_4N ($a = 3.857$ Å).

halide is reminiscent of our prior study on Cu_3N from $CuCl_2/NaN_3$ that showed some CuCl intermediate formation.[13] These results indicate that the azide formation process in superheated toluene requires several days of heating at elevated temperatures (~200 °C) to fully consume the stoichiometric NaN_3 and metal halide precursors. We are investigating the efficacy of using coordinating solvent additives to accelerate azide formation and shorten the overall nitride synthetic process.

Manganese Nitride Products. The manganese nitrides are the most thermally stable of the three nitrides in this synthetic study and have a range of known compositions and structures, including tetragonal $Mn_{1+x}N$ and Mn_3N_2, hexagonal $Mn_{2+x}N$, and cubic Mn_4N.[28,32] The nitrogen-rich phases are less thermally stable; for example, MnN decomposes by 480 °C, while Mn_4N survives to ~900 °C. Our nitrogen-rich azide precursor reactions yield a black nanocrystalline nitride product that is consistent with a tetragonally distorted rock salt structure for MnN (θ-phase $M_{1+x}N$, $x < 0.2$, Figure 4a, b).[24,32a,b] In contrast to the nickel and iron nitrides, the manganese nitride products exhibit much higher air and/or moisture sensitivity and were generally stored in inert atmosphere after isolation. IR analysis indicates that azide residues are effectively removed from the MnN product during the wash process (Supporting Information, Figure S1c). The methanol-washed manganese nitride powders decompose to MnO under argon flow TG-DTA to 1000 °C

(26) (a) Liu, Z. Q.; Leineweber, A.; Mitsuishi, K.; Furuya, K. *J. Mater. Sci.* **2006**, *41*, 2673. (b) Xu, Y.-H.; Hosein, S.; Judy, J. H.; Wang, J.-P. *J. Appl. Phys.* **2005**, *97*, 10F915. (c) Wang, X.; Zheng, W. T.; Tian, H. W.; Yu, S. S.; Xu, W.; Meng, S. H.; He, X. D.; Han, J. C.; Sun, C. Q.; Tay, B. K. *Appl. Surf. Sci.* **2003**, *220*, 30. (d) Gerardin, D.; Morniroli, J. P.; Michel, H.; Gantois, M. *J. Mater. Sci.* **1981**, *16*, 159.

(27) (a) Jack, K. *Acta Crystallogr.* **1950**, *3*, 392. (b) Ding, X.-Z.; Zhang, F.-M.; Yan, J.-S.; Shen, H.-L.; Wang, X.; Liu, X.-H.; Shen, D.-F. *J. Appl. Phys.* **1997**, *82*, 5154. (c) Wang, X.; Zheng, W. T.; Gao, L. J.; Wei, L.; Guo, W.; Bai, Y. B.; Fei, W. D.; Meng, S. H.; He, X. D.; Han, J. C. *J. Vac. Sci. Technol. A* **2003**, *21*, 983.

(28) Suzuki, K.; Morita, H.; Kaneko, T.; Yoshida, H.; Fujimori, H. *J. Alloys Compd.* **1993**, *201*, 11.

(29) Gallego, J. M.; Grachev, S. Y.; Borsa, D. M.; Ecija, D.; Miranda, R. *Phys. Rev. B* **2004**, *70*, 115417.

(30) (a) Eck, B.; Dronkowski, R.; Takahashi, M.; Kikkawa, S. *J. Mater. Chem.* **1999**, *9*, 1527. (b) Jacobs, H.; Rechenback, D.; Zachwieja, U. *J. Alloys Compd.* **1995**, *227*, 10.

(31) Bouchard, R. J.; Frederick, C. G.; Johnson, V. *J. Appl. Phys.* **1974**, *45*, 4067.

(32) (a) Leineweber, A.; Niewa, R.; Jacobs, H.; Kockelmann, W. *J. Mater. Chem.* **2000**, *10*, 2827. (b) Suzuki, K.; Kaneko, T.; Yoshida, H.; Obi, Y.; Fujimori, H.; Morita, H. *J. Alloys Compd.* **2000**, *306*, 66. (c) Yang, H.; Al-Brithen, H.; Trifan, E.; Ingram, D. C.; Smith, A. R. *J. Appl. Phys.* **2002**, *91*, 1053.

(Supporting Information, Figure S2) and powders left in ambient room atmosphere slowly lost MnN diffraction intensity, likely because of hydrolysis. EDS analysis of washed MnN powders shows that chlorine and sodium are not detectable above baseline noise. The washed product has an M:N molar ratio close to the ideal 1:1 value for MnN, but lower than ideal overall percentages indicate that significant oxygen content is present.

The feasibility of improving Mn−N precursor reactions using solvothermally heated pressed reagent pellets was examined. The reactor pressure showed several pressure "surges" near 230 and 255 °C, indicating rapid local decomposition events occur, but the pellets were generally intact when removed from the reactor. The crystalline product from this pellet reaction was different from that obtained from the stirred loose powder reaction, with the major peaks most closely corresponding to a mixture of tetragonal Mn_3N_2 and cubic Mn_4N phases (JCPDS No. 1-1158 Mn_3N_2; No. 1-1102 Mn_4N, Figure 4c-e).[24,32a,b] An approximate phase ratio based on XRD intensities suggests that this product is ∼75% Mn_3N_2 and ∼25% Mn_4N corresponding to an average composition of $Mn_{3.25}N_{1.75}$. This formula corresponds to an M:N ratio of 1:0.54, which is in surprisingly good agreement the M:N ratio from elemental analysis (Table 1). For pellet reaction products, manganese content by EDS ranged from ∼60−90 at % across the mixed phase sample, sodium was not detected, and chlorine was below 2 at % relative to manganese. Given that the detected phases from the pellet reaction are more nitrogen-deficient than MnN from the stirred powder reaction, it is possible that the pellet reactions were either incomplete or they produced higher local heating from exothermic SSM events that caused nitrogen loss during product formation.

Nitride Morphologies and Magnetic Properties. The particle sizes and shapes for the Ni_3N and Fe_2N products consist of aggregated particles in the range of ∼100−500 nm range that arrange into larger micrometer sized aggregates (Figure 5A,C). A few monolithic and fibrous regions are visible in the Fe_2N product. Higher resolution TEM images show that both Ni_3N and Fe_2N contain identifiable irregularly shaped particles ranging from ∼10−50 nm in diameter, which is close to the average XRD crystallite size (Figure 5B,D). Less dense regions around the particles might be due to organic surface coatings.

The Mn−N reactions performed under different conditions (stirred powders or pressed pellets) lead to some clear morphology differences. The powder reaction product contains mainly particles near 100 nm in size, interspersed with a few micrometer length rod-like structures with ∼150 nm diameters (Figure 6A). In contrast, the pressed pellets show a striated alignment of rod-like structures that is reminiscent of product morphologies sometimes observed for solvent-free exothermic SSM reactions.[33] The solvothermal azide formation/decomposition reactions occurring in the pellets may locally act like solvent-free SSM reactions with limited propagation because of the surrounding solvent. This could
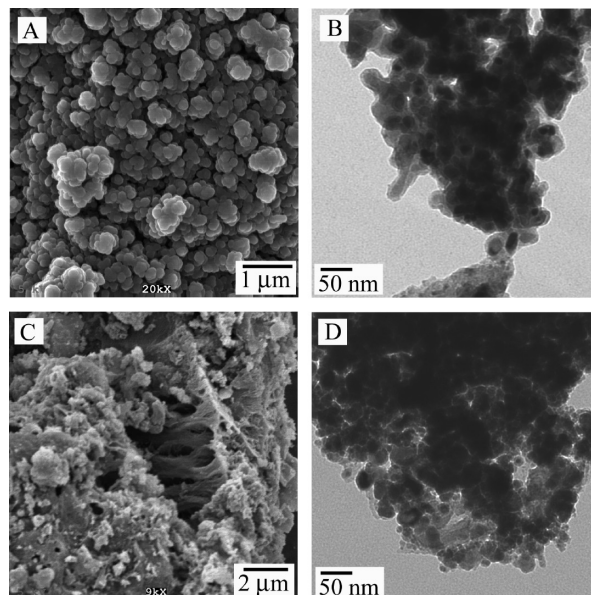
(33) Gillan, E. G.; Kaner, R. B. *J. Mater. Chem.* **2001**, *11*, 1951.

Figure 5. Scanning (left) and transmission (right) electron microscopy images for solvothermally produced Ni_3N (A, B) and Fe_2N (C, D).
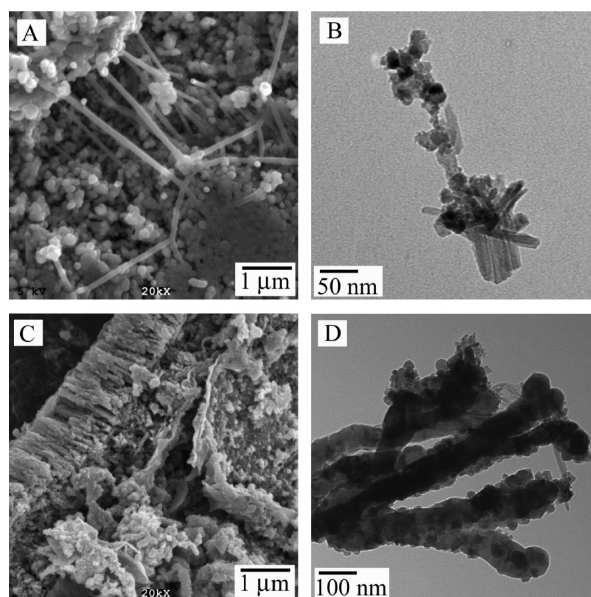

Figure 6. Scanning (left) and transmission (right) electron microscopy images for solvothermal products MnN (A, B) from powders and Mn_3N_2/Mn_4N mixture (C, D) from a pellet reaction.

aid in explaining the directional elongated morphologies inside the pellet. Under higher magnification TEM, both loose powder and pellet samples show evidence of particles around 20 nm in size, consistent with XRD crystallite size estimations, and rod-like formations, either as monolithic crystalline shards or as bent formations of aggregated particles (Figure 6B, D).

Late transition-metal nitrides exhibit a range of magnetic properties from diamagnetism, to paramagnetism or (anti)-ferromagnetism, depending on metal oxidation state, composition, structure, and crystallite size. Some metal-rich nitride thin films have found interest in high density magnetic recording media.[34] Ni_3N powder was found to act as a room temperature ferromagnet (T_c = 351 °C)[6b] and its films are described as strongly magnetic. Metal-rich Fe_xN ($x ≥ 2$)

materials are reportedly strongly magnetic or ferromagnetic at room temperature, agreeing with theoretical calculations.[9a,30,31,35] Our solvothermally synthesized Ni_3N and Fe_2N powders are strongly attracted to a permanent magnet through the walls of a glass vial. The measured room temperature gram susceptibility, χ_g, (molar susceptibility per mol metal, χ_m) for Ni_3N and Fe_2N are 2.44×10^{-4} cm^3/g (1.55×10^{-2} cm^3/mol Ni) and 1.90×10^{-3} cm^3/g (1.20×10^{-1} cm^3/mol Fe), respectively. Both of these values are much greater than the spin-only paramagnetic susceptibility calculated at 298 K assuming N^{3-} anions and a high spin metal ion environment, which for Ni^+ is 1.26×10^{-3} cm^3/mol Ni and for a 50/50 mix of Fe^{2+}/Fe^+ ions is 8.07×10^{-3} cm^3/mol Fe.

Some Mn−N phases, such as cubic MnN or tetragonal Mn_3N_2, exhibit antiferromagnetism with reported T_N values of 377 °C[36] and 652 °C,[6a] respectively. Metal-rich cubic Mn_4N reportedly shows net attractive ferrimagnetic ($T_N = 472$ °C) interactions.[37] The MnN solvothermal powder reaction product did not show visible attraction to a strong permanent magnet and had lower susceptibility ($\chi_g = 2.98 \times 10^{-5}$ cm^3/g, $\chi_m = 2.07 \times 10^{-3}$ cm^3/mol Mn) than that predicted for the spin only magnetic susceptibility of a high spin Mn^{3+} ion at 298 K (1.01×10^{-2} cm^3/mol). For the pellet reaction's mixed phase product (~75% Mn_3N_2 and 25% Mn_4N) only a fraction of the product powder was attracted to a permanent magnet and the powder's magnetic susceptibility ($\chi_g = 1.34 \times 10^{-4}$ cm^3/g, $\chi_m = 8.37 \times 10^{-3}$ cm^3/mol Mn based on 75:25 Mn_3N_2:Mn_4N molar ratio), consistent the presence of a minority ferromagnetic Mn_4N component. For reference, the measured susceptibility is near that calculated for a high spin paramagnetic Mn^{2+} ion (1.47×10^{-2} cm^3/mol). As noted earlier, the measured molar susceptibilities for all of these solvothermally synthesized metal nitrides should be regarded as higher than true values, since there are varying amounts of organic components that contribute to the overall sample mass; thus, actual metal contents are lower than the ideal nitride formulation.

Conclusions

The solvothermally moderated exothermic metathesis reactions between metal halides and NaN_3 produce several mid to late transition metal nitrides. The products are Ni_3N, Fe_2N, and MnN phases that are thermally metastable with respect to decomposition and nitrogen loss at moderate temperatures (<500 °C). The superheated toluene solvothermal environment slows decomposition of energetically unstable metal azide intermediates, producing nanocrystalline nitrides that form aggregated nanoparticulate structures. When the Mn−N solvothermal reaction was run with pressed pellets of the starting materials, the nitride product was more nitrogen poor with a more aggregated or striated morphology. This pellet reaction shows that the solvent surrounding the pellet is less able to prevent the exothermic metathesis reaction from overheating of the thermally sensitive nitride products as compared to stirred powder mixtures. The room temperature magnetic properties are consistent with magnetic properties determined for their bulk phase counterparts. This solvothermally moderated azide decomposition strategy may be applicable to the synthesis of more complex nitride structures such as transition metal doped nitride semiconductors.

Supporting Information Available: Solid-state transmission IR and TGA decomposition data for nitride products, XRD stack plot of Fe_2N thermal annealing products. This material is available free of charge via the Internet at http://pubs.acs.org.

IC900260U

(34) (a) Shinno, H.; Uehara, M.; Saito, K. *J. Mater. Sci.* **1997**, *32*, 2255. (b) Cao, M.; Liu, T.; Sun, G.; Wu, X.; He, X.; Hu, C. *J. Solid State Chem.* **2005**, *178*, 2390.
(35) Wang, X.; Zheng, W. T.; Tian, H. W.; Yu, S. S.; Xu, W.; Meng, S. H.; He, X. D.; Han, J. C.; Sun, C. Q.; Tay, B. K. *Appl. Surf. Sci.* **2003**, *220*, 30.
(36) Suzuki, K.; Suzuki, T.; Fujinaga, Y.; Kaneko, T.; Yoshida, H.; Obi, Y.; Tomiyoshi, S. *J. Alloys Compd.* **2003**, *360*, 34.
(37) Takei, W. J.; Heikes, R. R.; Shirane, G. *Phys. Rev.* **1962**, *125*, 1893.